

Probing Cosmic Curvature with Fast Radio Bursts and DESI DR2

Jéferson A. S. Fortunato ^{*}  ^{1,2,3,†} Wilian S. Hipólito-Ricaldi  ^{4,5,‡} and Gustavo E. Romero  ^{2,6,§}

¹*PPGCosmo, CCE, Universidade Federal do Espírito Santo (UFES),
Av. Fernando Ferrari, 540, CEP 29.075-910, Vitória, ES, Brazil*

²*Instituto Argentino de Radioastronomía, CCT La Plata,
CONICET; CICPBA; UNLP, C.C.5, (1894) Villa Elisa, Argentina*

³*High Energy Physics, Cosmology & Astrophysics Theory (HEPCAT) Group,
Department of Mathematics and Applied Mathematics,
University of Cape Town, Cape Town 7700, South Africa*

⁴*Departamento de Ciências Naturais, CEUNES, Universidade Federal
do Espírito Santo (UFES), Rodovia BR 101 Norte, km. 60,
CEP 29.932-540, São Mateus, ES, Brazil*

⁵*Núcleo Cosmo-UFES, CCE, Universidade Federal do Espírito Santo (UFES),
Av. Fernando Ferrari, 540, CEP 29.075-910, Vitória, ES, Brazil*

⁶*Facultad de Ciencias Astronómicas y Geofísicas,
Universidad Nacional de La Plata, B1900FWA La Plata, Argentina*

The spatial curvature of the Universe remains a central question in modern cosmology. In this work, we explore the potential of localized Fast Radio Bursts (FRBs) as a novel tool to constrain the cosmic curvature parameter Ω_k in a cosmological model-independent way. Using a sample of 80 FRBs with known redshifts and dispersion measures, we reconstruct the Hubble parameter $H(z)$ via artificial neural networks, which is then used to obtain angular diameter distances $D_A(z)$ through two complementary approaches. First, we derive the comoving distance $D_C(z)$ and $D_A(z)$ from FRBs without assuming a fiducial cosmological model. Then, the $H(z)$ reconstruction is combined with Baryon Acoustic Oscillation (BAO) measurements to infer $D_A(z)$. By comparing the FRB-derived and BAO+FRB-derived $D_A(z)$ values, we extract constraints on Ω_k under the Friedmann–Lemaître–Robertson–Walker metric. Our results show consistency with a spatially flat Universe within 1σ uncertainties, although a mild preference for negative curvature is observed across both covariance-based and Gaussian analyses. This study highlights the growing relevance of FRBs in precision cosmology and demonstrates their synergy with BAO data as a powerful probe of the large-scale geometry of the Universe.

Keywords: Fast Radio Bursts, Artificial Neural Networks, Cosmic Distances, Curvature of Universe.

I. INTRODUCTION

Determining the spatial geometry of the Universe through the curvature parameter Ω_k is a fundamental goal in cosmology. It directly impacts the measurement of distances, as well as our understanding of spacetime, the global topology of the Universe, its ultimate fate, and the physics of the early times, for instance.

The current constraints on Ω_k are largely consistent with flatness, although uncertainties remain. For instance, combining *Planck* Cosmic Microwave Background (CMB) lensing data with low-redshift Baryon Acoustic Oscillations (BAO) measurements yields $\Omega_k = 0.0007 \pm 0.0019$ [1]. However, other analyses challenge this result. Notably, [2] reported a preference for a mildly closed Universe, with $\Omega_k = -0.044^{+0.018}_{-0.015}$, based

solely on CMB temperature and polarization data from *Planck* satellite. Another study found a preference for a closed Universe at the 2σ confidence level, measuring $\Omega_k = -0.089^{+0.049}_{-0.046}$ when applying Effective Field Theories of Large Scale Structure (EFTofLSS) to BAO data [3]. On the other hand, [4] reported $\Omega_k = 0.108 \pm 0.056$, which is in 2.6σ tension with the CMB lensing data result. To obtain this estimate, they used a combination of datasets, including BAO, Cosmic Chronometers (CC), and Strong Gravitational Lensing (SGL).

However, it is important to recognize that these constraints are inherently cosmological model-dependent, relying on assumptions within the non-flat Λ CDM framework, which suffers from the well-known intrinsic degeneracy between cosmic curvature and the Hubble constant. Moreover, as with the Hubble tension, the apparent disagreement in curvature estimates raises the question of whether systematic biases or new physics are at play. In this context, exploring methods that provide a complementary and cosmological model-independent perspective is particularly valuable. Developing curvature measurements that are independent of the cosmological model, especially those that do not rely solely on CMB-based assumptions, offers a promising pathway to gaining a better understanding of these issues.

Recent studies [5, 6], which provide a methodological basis for the present work, have proposed model-

^{*}Corresponding author

[†]jeferson.fortunato@edu.ufes.br

[‡]wiliam.ricaldi@ufes.br

[§]romero@iar.unlp.edu.ar

independent approaches by combining BAO and Hubble parameter data. Although their methodologies are broadly similar, the former utilizes only BOSS and eBOSS BAO data and omits the covariance matrix, whereas the latter incorporates full covariance information and includes additional measurements from DESI DR1. Both studies find results consistent with flat spatial curvature within the reported uncertainties.

Extending these methodologies, we adopt a comparable framework to systematically assess the impact of including versus omitting the covariance matrix on cosmic curvature estimates. Additionally, we incorporate FRBs as novel and independent tracers to reconstruct the Hubble parameter $H(z)$, offering a complementary perspective to traditional probes such as supernovae or cosmic chronometers. This inclusion introduces a new observational channel based on dispersion measures, thereby enhancing the robustness and versatility of model-independent curvature constraints. We further combine this with the latest BAO data from BOSS, eBOSS, and DESI DR2 [7].

FRBs have emerged as a promising new probe in cosmology. These events are characterized by millisecond-duration and highly luminous pulses in the radio frequency spectrum. First discovered in 2007 by Lorimer et al. [8], FRBs exhibit large dispersion measures (DMs), that significantly exceed the expected contribution from the Milky Way. This excess provides strong evidence for their extragalactic, and potentially cosmological, origin [9]. Since that initial detection, hundreds of FRBs have been observed, and a subset has been precisely localized to host galaxies with measured redshifts [10].

Beyond their intriguing astrophysical nature, FRBs have proven to be valuable probes for cosmology. In particular, localized FRBs, those with measured redshifts and host galaxy associated, provide unique observational access to the otherwise elusive ionized content of the intergalactic medium (IGM). Over the past few years, multiple studies have employed these events to estimate key cosmological quantities, such as the Hubble constant H_0 [11–16], cosmographic parameters [17], the cosmic proper distance [18], the baryon fraction in the IGM [19–21], constrain dark energy equation of state [22, 23], trace the magnetic fields in the IGM [24], probe the equivalence principle [25–27], the rest mass of photons [28–30], to cite some.

In this work, we implement a method to determine the cosmic curvature by leveraging the synergy between FRBs and BAO measurements, with FRBs serving as the core observable. By comparing two estimates of the angular diameter distance $D_A(z)$, independently reconstructed from FRBs alone and from FRBs+BAO data sets, we infer Ω_k without relying on a specific cosmological model. This is made possible by using the FRB dispersion measure to reconstruct $H(z)$ through an artificial neural network algorithm, as demonstrated in [16] and to trace the comoving distance D_C via the integrated electron density along the line of sight.

We assume the validity of the Cosmological Principle, adopting the premise that the Universe is homogeneous and isotropic on large scales. Consequently, the background spacetime is described by the Friedmann–Lemaître–Robertson–Walker (FLRW) metric, with the curvature parameter Ω_k determining the geometry of the Universe: flat ($\Omega_k = 0$), open ($\Omega_k > 0$), or closed ($\Omega_k < 0$).

This paper is organized as follows: Section II describes some basic properties of FRBs. Section III presents an overview of distance calculations in cosmology within the FLRW framework. In Section IV we discuss the methodology used to reconstruct $H(z)$ and the comoving distance from FRB data, which are subsequently employed to infer the cosmic curvature density parameter. The data utilized in this work are detailed in Section V. Our results and discussion are presented in Section VI. Finally, Section VII contains our conclusions.

II. BASIC PROPERTIES OF FAST RADIO BURSTS

The observed dispersion measure, DM_{obs} , is the sum of local and extragalactic contributions, expressed as:

$$DM_{\text{obs}} = DM_{\text{local}} + DM_{\text{EG}}(z), \quad (1)$$

where the local component includes contributions from the Milky Way:

$$DM_{\text{local}} = DM_{\text{ISM}} + DM_{\text{halo}}, \quad (2)$$

and the extragalactic component includes contributions from the intergalactic medium (IGM) and the host galaxy of FRBs:

$$DM_{\text{EG}} = DM_{\text{IGM}} + \frac{DM_{\text{host}}}{(1+z)}. \quad (3)$$

Each term in this decomposition corresponds to distinct astrophysical environments. DM_{ISM} accounts for free electrons in the interstellar medium of the Milky Way and is commonly estimated using galactic electron density models like NE2001 [31] and YMW16 [32]. We adopt NE2001, as recent studies suggest that YMW16 may overestimate DM_{ISM} at low Galactic latitudes [33]. The Galactic halo contribution, DM_{halo} , is less constrained but estimated in the range $50 - 100 \text{ pc cm}^{-3}$ [34], based on observational constraints, such as the dispersion measure to the Large Magellanic Cloud (LMC), high-velocity cloud dynamics, and hydrostatic equilibrium models of the galactic halo gas. We then adopt a conservative value of $DM_{\text{halo}} = 50 \text{ pc cm}^{-3}$.

The intergalactic medium (IGM) dispersion measure, DM_{IGM} , dominates the observed DM_{obs} and is crucial for cosmology. However, DM_{IGM} exhibits significant scatter

due to electron distribution inhomogeneities along the line of sight. Its mean value is given by [35]:

$$\langle \text{DM}_{\text{IGM}} \rangle = \left(\frac{3c}{8\pi G m_p} \right) \Omega_b H_0 \int_0^z \frac{(1+z') f_{\text{IGM}}(z') f_e(z')}{E(z')} dz', \quad (4)$$

where c is the speed of light, G the gravitational constant, and m_p the proton mass. Ω_b is the cosmic baryon density, and $E(z) = H(z)/H_0$ the normalized Hubble parameter. The term $f_{\text{IGM}}(z)$ denotes the baryon fraction in the intergalactic medium, which we take as $f_{\text{IGM}} = 0.82 \pm 0.04$ [36, 37]. The factor $f_e(z)$ describes the baryons ionization state and is defined as:

$$f_e(z) = Y_H X_{e,H}(z) + \frac{1}{2} Y_{\text{He}} X_{e,\text{He}}(z), \quad (5)$$

where $Y_H = 0.75$ and $Y_{\text{He}} = 0.25$ are the mass fractions of hydrogen and helium, respectively. The terms $X_{e,H}(z)$ and $X_{e,\text{He}}(z)$ denote their ionization fractions. Since both are fully ionized at $z < 3$, we set $X_{e,H} = X_{e,\text{He}} = 1$.

The host galaxy contribution, DM_{host} , depends on the local environment of the FRB and varies with redshift due to cosmological expansion. Although some studies assume a constant value (for example, $\text{DM}_{\text{host}} = 100 \text{ pc cm}^{-3}$ [38]), this can yield unphysical results at low redshifts, including DM_{IGM} negative values. To address this issue, we adopt the redshift-dependent parametrization proposed by [39], based on the IllustrisTNG simulation:

$$\text{DM}_{\text{host}} = A(1+z)^\alpha, \quad (6)$$

where A and α are free parameters that depend on the FRB type and host galaxy properties. For instance, repeating FRBs in spiral galaxies follow $\text{DM}_{\text{host}} = 34.72(1+z)^{1.08} \text{ pc cm}^{-3}$, while non-repeating ones follow $\text{DM}_{\text{host}} = 32.97(1+z)^{0.84} \text{ pc cm}^{-3}$.

The decomposition in Eq. (1) isolates DM_{IGM} , which is crucial for using FRBs as cosmological probes, as discussed in the following sections.

III. DISTANCES IN COSMOLOGY

The comoving distance D_C is a key cosmological quantity, providing an invariant measure of spatial separation between an observer and a distant object, independent of cosmological expansion. In the FLRW framework, D_C is defined as:

$$D_C(z) = c \int_0^z \frac{dz'}{H(z')}. \quad (7)$$

A related quantity is the horizon distance D_H , which represents the maximum scale over which information could have been exchanged since the Big Bang. It is defined as:

$$D_H = \frac{c}{H_0}. \quad (8)$$

This distance sets a fundamental scale in cosmology and is often used to normalize other cosmological distances.

On the other hand, the metric distance D_M is related to the comoving distance and depends on the curvature. For different values of the curvature parameter Ω_k , its functional form is [40]:

$$D_M = \begin{cases} \frac{D_H}{\sqrt{\Omega_k}} \sinh \left(\sqrt{\Omega_k} \frac{D_C}{D_H} \right), & \text{if } \Omega_k > 0, \\ D_C, & \text{if } \Omega_k = 0, \\ \frac{D_H}{\sqrt{|\Omega_k|}} \sin \left(\sqrt{|\Omega_k|} \frac{D_C}{D_H} \right), & \text{if } \Omega_k < 0, \end{cases} \quad (9)$$

where $\Omega_k = 0$ for a flat universe, $\Omega_k > 0$ for an open universe and $\Omega_k < 0$ for a closed universe.

In observational cosmology, absolute distance measurements are difficult to obtain; instead, dimensionless ratios normalized by the sound horizon r_d are commonly used. Two ratios frequently used in BAO analysis are:

$$\frac{D_M(z)}{r_d}, \quad \text{and} \quad \frac{D_H(z)}{r_d}. \quad (10)$$

The sound horizon r_d , is the maximum distance that acoustic waves could travel in the primordial plasma before photon decoupling and is given by [41]:

$$r_d = \int_{z_d}^{\infty} \frac{c_s dz}{H(z)}, \quad (11)$$

where c_s is the speed of sound in the primordial plasma and z_d denotes the baryon drag redshift, corresponding to the epoch when baryons decoupled from radiation. Measuring the scale r_d from BAO data provides an independent way to test cosmological models and infer the universe's expansion rate.

The quantities D_M/r_d and D_H/r_d serve as angular and radial standard rulers, respectively. D_M/r_d determines the angular scale of BAO features in galaxy distributions, while D_H/r_d determines the radial scale of the BAO peak in redshift-space distortions. BAO surveys measure the peak in both directions: perpendicular and along the line of sight, tracing D_M/r_d and D_H/r_d , respectively. This dual measurement provides constraints on the expansion history $H(z)$ and the curvature parameter Ω_k , offering an independent probe of the cosmological model.

In practice, the metric distance is not directly observable. Instead, we measure the angular diameter distance D_A . Due to cosmic expansion, D_A is related to the comoving transverse distance D_M by:

$$D_A(z) = \frac{D_M(z)}{1+z}. \quad (12)$$

By combining distance ratios D_M/r_d and r_d/D_H , we obtain an expression for D_A that depends only on observational quantities [5, 6]:

$$D_A(z) = \frac{c}{(1+z)H(z)} \frac{D_M}{r_d} \frac{r_d}{D_H}. \quad (13)$$

This formulation is useful for inferring D_A in a model-independent way, relying solely on measurements of the Hubble parameter and BAO-derived distance ratios. It enables cosmological tests without assuming a specific value of r_d , making it robust to uncertainties in early-universe physics. We will use this equation later to combine FRBs and BAO data in section VI.

IV. METHODOLOGY

Following the discussions in the previous sections, we now describe the reconstruction of the comoving distance using real FRB data and its integration with BAO measurements. This section also outlines the technical procedures to derive angular diameter distances and constrain the curvature.

A. Extracting D_C and D_A from $\langle \text{DM}_{\text{IGM}} \rangle$

To infer the comoving distance from the dispersion measure, we rewrite the Macquart relation, i.e., Eq.(4), as:

$$\langle \text{DM}_{\text{IGM}}(z) \rangle = A \int_0^z F(z') \dot{D}_C(z') dz', \quad (14)$$

with

$$A = \frac{3c\Omega_b H_0^2}{8\pi G m_p}, \quad (15)$$

where the free electron distribution in the IGM introduces an additional modulation described by the function:

$$F(z) = (1+z)f_{\text{IGM}}(z)f_e(z), \quad (16)$$

and $\dot{D}_C(z) = dD_C(z)/dz$.

The redshift-dependent factor $F(z)$ must be removed from $\langle \text{DM}_{\text{IGM}} \rangle$. This is done by differentiating Eq. (14) with respect to redshift (note that Eq. (7) was also derived.)

$$\dot{D}_C(z) = \frac{c}{H(z)} = \frac{1}{AF(z)} \frac{d\langle \text{DM}_{\text{IGM}}(z) \rangle}{dz}, \quad (17)$$

and then integrating $c/H(z)$, thus yielding a direct estimate of D_C from the FRB data.

The key step in reconstructing D_C is obtaining the derivative $d\langle \text{DM}_{\text{IGM}}(z) \rangle (dz)^{-1}$. Although this method

was first proposed in [18], the lack of a sufficient number of localized FRBs at the time led to the use of simulations and Gaussian Processes. In contrast, here we apply the method to real data, using artificial neural networks (ANNs) to reconstruct the derivative and constrain cosmic curvature. In particular, we use the method developed in [16], in which ANNs are trained to reconstruct the relation between DM_{IGM} and z in a data-driven manner.

Specifically, we adopted a Multilayer Perceptron (MLP) architecture implemented using the `scikit-learn` library [42], applying hyperparameter tuning via `GridSearchCV` to identify the optimal model. Various configurations of hidden layer sizes, activation functions, solvers, and learning rates were tested. The optimal model was selected based on cross-validation performance and learning curve analysis, ensuring that overfitting was minimized and that the network generalizes well to unseen data (see [16] for more details). Bootstrap resampling was used to estimate uncertainties in the ANNs predictions, enabling robust error propagation to the reconstructed derivative $\frac{d\langle \text{DM}_{\text{IGM}} \rangle}{dz}$ and, consequently, to $D_C(z)$.

Once $D_C(z)$ is known, the angular diameter distance can be derived solely from the FRB data using Eqs. (9) and (12). From now on, we refer to the $D_A(z)$ obtained exclusively from FRB data as $D_A^{\text{FRB}}(z)$. It is important to emphasize that the determination of both $D_C(z)$ and $D_A^{\text{FRB}}(z)$ is entirely independent of any cosmological model and is derived directly from the data.

B. Estimation of the cosmic curvature

The key aspect of our approach to constraining spatial curvature is that FRBs play a dual role in the process. First, as described above, they allow us to directly obtain $D_A^{\text{FRB}}(z)$ from the data. Second, as demonstrated in [16], the quantity $\left(\frac{d\langle \text{DM}_{\text{IGM}}(z) \rangle}{dz} \right)^{-1}$ enables the reconstruction of $H(z)$ and H_0 — see Eq. (17). The Hubble parameter derived from FRBs can also be combined with BAO measurements of the ratios D_M/r_d and D_H/r_d , enabling the determination of the angular diameter distance via Eq. (13) in a cosmology-independent manner, using only the data. We shall refer to the angular diameter distance obtained in this way as $D_A^{\text{BAO+FRB}}(z)$.

This approach allows us to compare $D_A^{\text{FRB}}(z)$ and $D_A^{\text{BAO+FRB}}(z)$ to estimate the spatial curvature parameter Ω_k in a data-driven manner. In both cases of D_A estimation, the Hubble constant H_0 is not externally imposed but is self-consistently derived by extrapolating the FRB-based reconstruction of $H(z)$ to redshift $z = 0$. This internal determination of H_0 helps mitigate the degeneracy between H_0 and Ω_k , avoiding the need for external priors that could bias their coupling. Moreover, since H_0 enters both D_A and D_C symmetrically, variations in its value do not affect the determination of Ω_k .

within this framework.

To constrain Ω_k , we implement two distinct approaches:

- **Covariance matrix approach:** In our first approach, we account for the statistical correlation among the distance data points, primarily because both the angular diameter distance $D_A(z)$ and the comoving distance $D_C(z)$ depend on the same reconstructed Hubble parameter $H(z)$. To properly account for these correlations in the likelihood analysis, we construct a covariance matrix that incorporates both statistical uncertainties and correlated terms, following the strategy proposed in [6]. The likelihood function is given by

$$\ln \mathcal{L} = -\frac{1}{2} \Delta D_i^T \mathbf{Cov}_{ij}^{-1} \Delta D_j, \quad (18)$$

where the residuals are defined as $\Delta D = D_A^{\text{BAO+FRB}}(z_i) - D_A^{\text{FRB}}(z_i; \Omega_k)$, and the total covariance matrix is expressed as

$$\mathbf{Cov}_{ij} = \mathbf{Cov}_{ii}^{\text{stat}} + \mathbf{Cov}_{ij}^{\text{corr}}. \quad (19)$$

The statistical part captures the propagated uncertainties from the reconstruction of $H(z)$ and the BAO-based measurements. The correlated term reflects the intrinsic coupling between D_A and D_C , since both quantities are derived from the same FRB-based estimates of $H(z)$. This term is computed using the standard definition of covariance: $\text{Cov}(X_i, Y_j) = \mathbb{E}[(X_i - \mu_i)(Y_j - \mu_j)]$.

Although the DESI collaboration provides a fiducial covariance matrix, it is derived under specific model assumptions and tailored to their reconstruction method. In contrast, our analysis relies on a model-independent reconstruction of $H(z)$ and therefore requires a covariance matrix that accurately reflects our methodology. By constructing the covariance matrix directly from our reconstructed distances, we ensure internal consistency and avoid potential mismatches. Moreover, the authors in [6] have shown that this method yields results consistent with the DESI covariance estimates, further supporting the reliability of this approach.

- **Gaussian χ^2 approach:** For comparison, we also implement a simpler approach in which all data points are treated as independent and Gaussian-distributed. In this case, we use the traditional χ^2 minimization method:

$$\chi^2 = \sum_i \frac{[D_A^{\text{BAO+FRB}}(z_i) - D_A^{\text{FRB}}(z_i; \Omega_k)]^2}{\sigma_i^2}, \quad (20)$$

where σ_i represents the combined error from the reconstruction of D_A and D_C . This method does not account for correlations among the data points and may underestimate the uncertainty, but it serves as a useful baseline.

V. DATA

To implement our analysis, we use a subset of 80 from the 92 localized FRBs compiled by [43]. In addition to requiring known redshifts and dispersion measures, we impose a selection criterion also introduced in [43] to ensure the physical consistency of the intergalactic medium contribution to the dispersion measure, DM_{IGM} . Specifically, we require

$$\text{DM}_{\text{obs}} - \text{DM}_{\text{MW}} > 80 \text{ pc cm}^{-3},$$

which accounts for a typical range of halo contributions, $\text{DM}_{\text{halo}} \sim 50\text{--}80 \text{ pc cm}^{-3}$. This criterion serves as a practical proxy to enforce $\text{DM}_{\text{obs}} - \text{DM}_{\text{MW}} - \text{DM}_{\text{halo}} > 0$, ensuring that the inferred DM_{IGM} remains physically meaningful and avoids negative values. This cut also helps to eliminate FRBs with low total extragalactic dispersion, which could lead to biased inferences of the Hubble parameter, particularly by favouring artificially high values of H_0 within a narrow prior range, as shown in [43]. Furthermore, this selection indirectly filters out several low-redshift FRBs that may be heavily influenced by peculiar velocities of their host galaxies and the local cosmic web. By excluding these events, we minimize the impact of non-cosmological effects on the reconstruction of $H(z)$ and improve the robustness of the derived distances.

In addition, seven events were excluded from our analysis for specific reasons. First, FRB200110E is omitted because it is located at an extremely close distance of only 3.6 Mpc, within a globular cluster in the M81 galaxy [51, 52]. Its proximity implies a negligible contribution from the intergalactic medium, making it unsuitable for cosmological inference. Second, FRB210117 and FRB190520 display dispersion measures significantly exceeding theoretical expectations based on their redshift. These anomalies classify them as statistical outliers, probably influenced by a dense or highly magnetized local environment in their host galaxy [53–55]. Moreover, we did not reconstruct the functions at higher redshift values due to the lack of FRB data points in this regime. Although there are four points around $z \sim 1$ — FRB220610, FRB221029, FRB230521, FRB240123 — we excluded them because they could bias the reconstruction, given the gap between them and the last point used in this study at $z = 0.66$. The remaining 80 FRBs form a clean and physically consistent dataset for the curvature analysis presented in the following sections.

For the analysis that follows, we employ a total of ten BAO data points in the range of the reconstructed FRBs redshifts, $z = [0, 1.5]$: five from the BOSS/eBOSS programs and five from the recent DESI DR2 release, summarized in Table I. These measurements are used in combination with our FRB and ANN-based reconstructions of $H(z)$ and distances, to constrain the cosmic curvature parameter Ω_k .

Data source	z	D_M/r_d	D_H/r_d	Ref.
BOSS galaxy-galaxy	0.38	10.23 ± 0.17	25.00 ± 0.76	[44]
eBOSS galaxy-galaxy	0.51	13.36 ± 0.21	22.33 ± 0.58	[44]
eBOSS galaxy-galaxy	0.70	17.86 ± 0.33	19.33 ± 0.62	[45, 46]
eBOSS galaxy-galaxy	0.85	19.60 ± 0.41	19.60 ± 0.72	[47, 48]
eBOSS galaxy-galaxy	1.48	30.21 ± 0.79	13.23 ± 0.47	[49, 50]
DESI DR2 LRG1	0.510	13.588 ± 0.167	21.863 ± 0.425	[7]
DESI DR2 LRG2	0.706	17.351 ± 0.177	19.455 ± 0.330	[7]
DESI DR2 LRG3+ELG1	0.934	21.576 ± 0.152	17.641 ± 0.193	[7]
DESI DR2 ELG2	1.321	27.601 ± 0.318	14.176 ± 0.221	[7]
DESI DR2 QSO	1.484	30.512 ± 0.760	12.817 ± 0.516	[7]

TABLE I: Measurements of D_M/r_d and D_H/r_d from various surveys.

VI. RESULTS AND DISCUSSIONS

To apply the methodology described above, we first subtract the contributions from the Milky Way, the halo, and the host galaxy in order to obtain DM_{IGM} from the observed dispersion measures of the subset of 80 FRBs described in Sec. V. Then we reconstruct the comoving distance $D_C(z)$. The first step involves determining the redshift evolution of the average intergalactic dispersion measure, $\langle \text{DM}_{\text{IGM}}(z) \rangle$. As detailed in Sec. IV, this is performed using an ANN algorithm (see [16] for more details). The result is shown in panel (a) in Figure 1. The red points with error bars represent the individual FRB measurements and their associated uncertainties, while the solid black curve corresponds to the ANN-based reconstruction. The shaded region around it denotes the 1σ confidence interval.

Once $\langle \text{DM}_{\text{IGM}}(z) \rangle$ is reconstructed, it is used to derive the comoving distance $D_C(z)$ (see Eq. (17)). The resulting comoving distance curve is displayed in panel (b) in Figure 1. The dashed black line shows the reconstructed $D_C(z)$, while the shaded blue band represents the associated 1σ uncertainty. This reconstruction provides a continuous cosmological model-independent estimate of the comoving distance across a range of redshifts, from low redshifts up to $z \sim 1.5$, where BAO measurements are also available for comparison. Subsequently, $D_A^{\text{FRB}}(z)$ and $D_A^{\text{BAO+FRB}}(z)$ are computed.

To constrain Ω_k , we explore the likelihood using the `emcee` Python module, a Markov Chain Monte Carlo (MCMC) ensemble sampler [56]. The prior for the Hubble constant is taken as the extrapolated value $H_0 = H(z = 0)$, obtained from the ANN reconstruction of the FRB data. The final results from both approaches (covariance matrix and χ^2 minimization) are presented and compared in Table II, and the corresponding posterior distributions are shown in Figure 2. These results demonstrate that the combined use of FRBs and BAO data provides a robust and independent constraint on the spatial geometry of the Universe.

From the covariance-based analysis (Table II), we derive the following constraints:

- The eBOSS data yield $\Omega_k = -0.25^{+0.35}_{-0.46}$, indicating a mild preference for a closed Universe, albeit with

Survey	Ω_k (with covariance)	Ω_k (without covariance)
eBOSS	$-0.25^{+0.35}_{-0.46}$	-0.18 ± 0.20
DESI DR2	$0.10^{+0.33}_{-0.38}$	-0.19 ± 0.08
eBOSS + DESI DR2	$-0.09^{+0.24}_{-0.31}$	-0.17 ± 0.06

TABLE II: Estimated values of the cosmic curvature parameter Ω_k using BAO and FRB comoving distance measurements.

substantial uncertainties.

- The DESI data alone provide a constraint centered around spatial flatness, with $\Omega_k = 0.10^{+0.33}_{-0.38}$.
- When combining the eBOSS and DESI DR2 datasets, the inferred curvature is $\Omega_k = -0.09^{+0.24}_{-0.31}$, suggesting a slightly closed Universe with reduced uncertainties compared to individual datasets.

In contrast, neglecting the off-diagonal elements of the covariance matrix (Table II) yields significantly tighter posterior distributions:

- For eBOSS, we find $\Omega_k = -0.18 \pm 0.20$,
- For DESI, $\Omega_k = -0.19 \pm 0.08$, and
- For the joint eBOSS + DESI DR2 analysis, $\Omega_k = -0.17 \pm 0.06$.

Despite variations in central values, all estimates remain consistent with a spatially flat Universe ($\Omega_k = 0$) at the 1σ level. The integration of FRB-based comoving distance reconstruction serves as an independent and complementary cosmological probe, reinforcing the growing utility of FRBs in precision cosmology.

Taken together, these results demonstrate that ANN reconstructions of comoving distances from FRBs, when combined with state-of-the-art BAO measurements, provide competitive constraints on spatial curvature, comparable to those obtained from other late-time cosmological probes [5, 6, 57, 58]. While Gaussian-based methods yield tighter intervals, they may underestimate uncertainties due to neglected correlations. The apparent preference for negative values in this case may result from omitting the covariance matrix, which can bias the final result. In contrast, the approach that incorporates

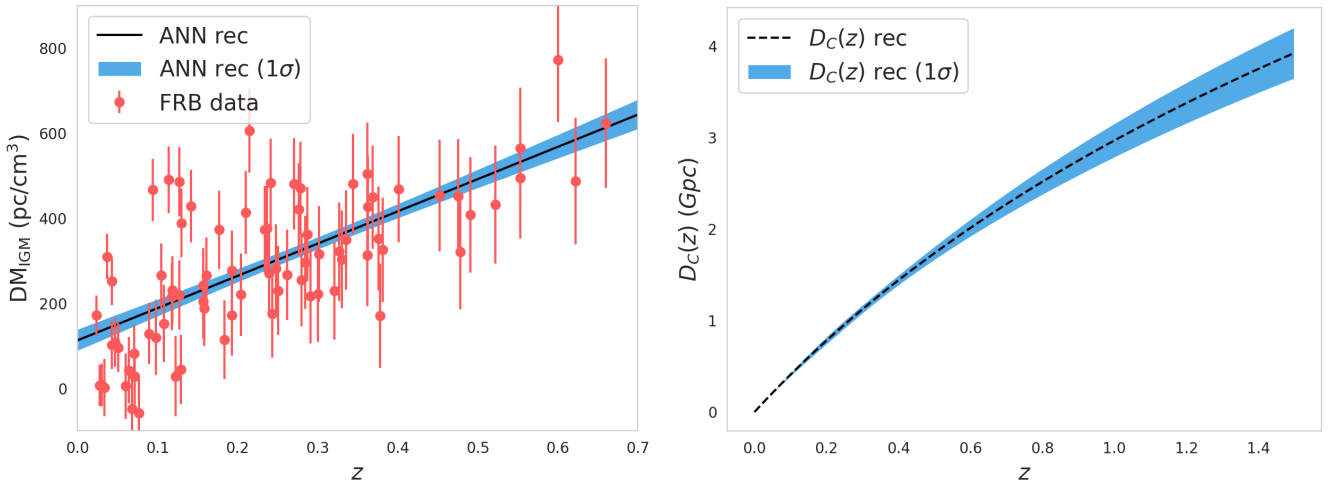


FIG. 1: Reconstructed FRBs observables. Left: redshift evolution of the average IGM dispersion measure $\langle DM_{IGM}(z) \rangle$. Right: comoving distance $D_C(z)$ inferred from FRBs.

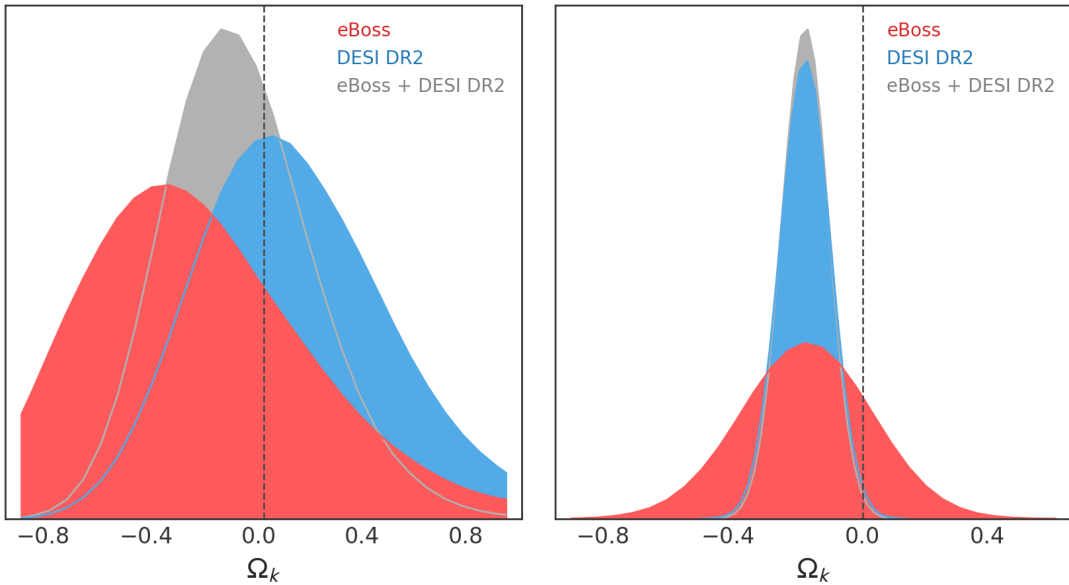


FIG. 2: Posterior probability distributions for the cosmic curvature parameter Ω_k under two assumptions. Left: using the full covariance matrix Right: Neglecting correlations.

the full covariance matrix, though yielding broader confidence regions, provides a more conservative and robust assessment of parameter uncertainties. These findings highlight the critical role of accounting for the full covariance structure in cosmological parameter inference, especially when combining different datasets or when intrinsic correlations are present.

It is worth noting, however, that across both methods, all central estimates of Ω_k lie on the negative side — except for DESI DR2, considering the covariance matrix —, indicating a mild but noticeable preference for a spatially closed Universe. While not statistically significant at the $> 2\sigma$ level, this trend persists across independent recon-

structions and may become more conclusive with future data. Overall, our findings support the consistency of current data with a spatially flat Universe, within $1-2\sigma$ across all analyses. The synergy between FRB-based reconstructions and BAO observations further underscores the emerging potential of FRBs as reliable cosmological tools.

VII. CONCLUSIONS

In this work, we presented a fully data-driven strategy to constrain the spatial curvature of the Universe

by leveraging the synergy between FRBs and BAO measurements. Reconstructing the Hubble parameter $H(z)$ using an ANN trained on a set of localized FRBs, we derived the comoving distance $D_C(z)$ and subsequently estimated $D_A(z)$ to compare with the same quantity obtained from BAO+FRB data. This dual-path approach enabled robust constraints on the curvature parameter Ω_k , independent of early-universe assumptions or fiducial cosmological models.

Our results indicate that, within current observational limits, all estimates remain consistent with a spatially flat Universe. However, a persistent mild preference for negative curvature is observed across multiple statistical treatments, suggesting that future improvements in data quantity and quality could be decisive. Incorporating the full covariance matrix in the likelihood analysis yields more conservative yet reliable uncertainty estimates, underscoring the importance of properly accounting for statistical correlations in precision cosmology.

Looking ahead, enhancing the constraining power of FRB-based curvature measurements will require advances on both observational and methodological fronts. Increasing the number of localized FRBs with secure redshift determinations will reduce statistical uncertainties and improve redshift coverage. The number of FRBs detected is indeed rapidly increasing with the advent of large-scale radio surveys and real-time localization capabilities, such as the Canadian Hydrogen Intensity Mapping Experiment (CHIME) [59], the Australian Square Kilometre Array Pathfinder (ASKAP) [60], the improved

version of the Karoo Array Telescope (MeerKAT) [61]. At the same time, improved modeling of host galaxy and halo contributions to the dispersion measure will mitigate systematic errors in the extraction of DM_{IGM} . On the analytical side, incorporating hybrid inference techniques that combine neural networks with advanced statistical frameworks may enhance the reconstruction accuracy and stability.

As new FRBs discoveries expand the redshift baseline and improve the resolution of the available datasets, their integration with BAO measurements promises to yield increasingly precise and independent insights into the geometry of the cosmos. This work reinforces the case for FRBs as a valuable cosmological probe and sets the stage for their broader inclusion in future large-scale structure analyses.

Acknowledgments

JASF thanks FAPES for their financial support. WSHR acknowledges partial financial support from FAPES. G.E.R. acknowledges financial support from the State Agency for Research of the Spanish Ministry of Science and Innovation under grant PID2022-136828NB-C41/AEI/10.13039/501100011033/, and by “ERDF A way of making Europe”, by the “European Union”. He also thanks support from PIP 0554 (CONICET).

[1] N. Aghanim, Y. Akrami, M. Ashdown, J. Aumont, C. Baccigalupi, M. Ballardini, A. Banday, R. Barreiro, N. Bartolo, S. Basak, *et al.*, *Astronomy & Astrophysics* **641**, A6 (2020).

[2] E. Di Valentino, A. Melchiorri, and J. Silk, *Nature Astronomy* **4**, 196 (2020).

[3] A. Glanville, C. Howlett, and T. Davis, *Monthly Notices of the Royal Astronomical Society* **517**, 3087 (2022).

[4] P.-J. Wu and X. Zhang, arXiv preprint arXiv:2411.06356 (2024).

[5] X. Gong, Y. Xu, T. Liu, S. Cao, J. Jiang, Y. Nan, R. Ding, and J. Wang, *Physics Letters B* **853**, 138699 (2024).

[6] T. Liu, S. Wang, H. Wu, S. Cao, and J. Wang, *The Astrophysical Journal Letters* **981**, L24 (2025).

[7] M. A. Karim, J. Aguilar, S. Ahlen, S. Alam, L. Allen, C. A. Prieto, O. Alves, A. Anand, U. Andrade, E. Armengaud, *et al.*, arXiv preprint arXiv:2503.14738 (2025).

[8] D. R. Lorimer, M. Bailes, M. A. McLaughlin, D. J. Narkevic, and F. Crawford, *Science* **318**, 777 (2007).

[9] E. Petroff, J. Hessels, and D. Lorimer, *The Astronomy and Astrophysics Review* **27**, 1 (2019).

[10] D. Zhou, J. Han, B. Zhang, K. Lee, W. Zhu, D. Li, W. Jing, W.-Y. Wang, Y. Zhang, J. Jiang, *et al.*, *Research in Astronomy and Astrophysics* **22**, 124001 (2022).

[11] J.-P. Macquart, J. Prochaska, M. McQuinn, K. Bannister, S. Bhandari, C. Day, A. Deller, R. Ekers, C. James, L. Marnoch, *et al.*, *Nature* **581**, 391 (2020).

[12] Q. Wu, G.-Q. Zhang, and F.-Y. Wang, *Monthly Notices of the Royal Astronomical Society: Letters* **515**, L1 (2022).

[13] Z.-W. Zhao, J.-G. Zhang, Y. Li, J.-M. Zou, J.-F. Zhang, and X. Zhang, arXiv preprint arXiv:2212.13433 (2022).

[14] S. Kalita, S. Bhatporia, and A. Weltman, *Physics of the Dark Universe* , 101926 (2025).

[15] S. Hagstotz, R. Reischke, and R. Lilow, *Monthly Notices of the Royal Astronomical Society* **511**, 662 (2022).

[16] J. A. Fortunato, D. J. Bacon, W. S. Hipólito-Ricaldi, and D. Wands, *Journal of Cosmology and Astroparticle Physics* **2025**, 018 (2025).

[17] J. A. Fortunato, W. S. Hipólito-Ricaldi, and M. V. dos Santos, *Monthly Notices of the Royal Astronomical Society* **526**, 1773 (2023).

[18] H. Yu and F. Wang, *Astronomy & Astrophysics* **606**, A3 (2017).

[19] Z. Li, H. Gao, J.-J. Wei, Y.-P. Yang, B. Zhang, and Z.-H. Zhu, *Monthly Notices of the Royal Astronomical Society: Letters* **496**, L28 (2020).

[20] K. Yang, Q. Wu, and F. Wang, *The Astrophysical Journal Letters* **940**, L29 (2022).

[21] T. Lemos, R. S. Gonçalves, J. C. Carvalho, and J. S. Alcaniz, arXiv preprint arXiv:2205.07926 (2022).

[22] B. Zhou, X. Li, T. Wang, Y.-Z. Fan, and D.-M. Wei, *Phys. Rev. D* **89**, 107303 (2014), arXiv:1401.2927 [astro-

ph.CO] .

[23] H. Gao, Z. Li, and B. Zhang, *Astrophys. J.* **788**, 189 (2014), arXiv:1402.2498 [astro-ph.CO] .

[24] T. Akahori, D. Ryu, and B. M. Gaensler, *Astrophys. J.* **824**, 105 (2016), arXiv:1602.03235 [astro-ph.CO] .

[25] J.-J. Wei, H. Gao, X.-F. Wu, and P. Mészáros, *Phys. Rev. Lett.* **115**, 261101 (2015), arXiv:1512.07670 [astro-ph.HE] .

[26] S. J. Tingay and D. L. Kaplan, *ApJ* **820**, L31 (2016), arXiv:1602.07643 [astro-ph.CO] .

[27] A. Nusser, *ApJ* **821**, L2 (2016), arXiv:1601.03636 [astro-ph.CO] .

[28] X.-F. Wu, S.-B. Zhang, H. Gao, J.-J. Wei, Y.-C. Zou, W.-H. Lei, B. Zhang, Z.-G. Dai, and P. Mészáros, *ApJ* **822**, L15 (2016), arXiv:1602.07835 [astro-ph.HE] .

[29] L. Shao and B. Zhang, *Phys. Rev. D* **95**, 123010 (2017), arXiv:1705.01278 [hep-ph] .

[30] H.-N. Lin, L. Tang, and R. Zou, *MNRAS* **520**, 1324 (2023), arXiv:2301.12103 [gr-qc] .

[31] J. M. Cordes and T. J. W. Lazio, arXiv preprint astro-ph/0207156 (2002).

[32] J. Yao, R. Manchester, and N. Wang, *The Astrophysical Journal* **835**, 29 (2017).

[33] S. K. Ocker, J. M. Cordes, and S. Chatterjee, *Astrophys. J.* **911**, 102 (2021), arXiv:2101.04784 [astro-ph.GA] .

[34] J. X. Prochaska and Y. Zheng, *Monthly Notices of the Royal Astronomical Society* **485**, 648 (2019).

[35] W. Deng and B. Zhang, *The Astrophysical Journal Letters* **783**, L35 (2014).

[36] J. M. Shull, B. D. Smith, and C. W. Danforth, *The Astrophysical Journal* **759**, 23 (2012).

[37] B. Zhou, X. Li, T. Wang, Y.-Z. Fan, and D.-M. Wei, *Physical Review D* **89**, 107303 (2014).

[38] S. P. Tendulkar, C. Bassa, J. M. Cordes, G. C. Bower, C. J. Law, S. Chatterjee, E. A. Adams, S. Bogdanov, S. Burke-Spoliar, B. J. Butler, *et al.*, *The Astrophysical Journal Letters* **834**, L7 (2017).

[39] G. Zhang, H. Yu, J. He, and F. Wang, *The Astrophysical Journal* **900**, 170 (2020).

[40] S. Weinberg, *Gravitation and cosmology: principles and applications of the general theory of relativity* (1972).

[41] L. E. Padilla, L. O. Tellez, L. A. Escamilla, and J. A. Vazquez, *Universe* **7**, 213 (2021).

[42] F. Pedregosa, G. Varoquaux, A. Gramfort, V. Michel, B. Thirion, O. Grisel, M. Blondel, P. Prettenhofer, R. Weiss, V. Dubourg, *et al.*, *the Journal of machine Learning research* **12**, 2825 (2011).

[43] Y.-Y. Wang, S.-J. Gao, and Y.-Z. Fan, arXiv preprint arXiv:2501.09260 (2025).

[44] S. Alam, M. Ata, S. Bailey, F. Beutler, D. Bizyaev, J. A. Blazek, A. S. Bolton, J. R. Brownstein, A. Burden, C.-H. Chuang, *et al.*, *Monthly Notices of the Royal Astronomical Society* **470**, 2617 (2017).

[45] J. E. Bautista, R. Paviot, M. Vargas Magaña, S. de La Torre, S. Fromenteau, H. Gil-Marín, A. J. Ross, E. Burtin, K. S. Dawson, J. Hou, *et al.*, *Monthly Notices of the Royal Astronomical Society* **500**, 736 (2021).

[46] H. Gil-Marín, J. E. Bautista, R. Paviot, M. Vargas Magaña, S. de La Torre, S. Fromenteau, S. Alam, S. Ávila, E. Burtin, C.-H. Chuang, *et al.*, *Monthly Notices of the Royal Astronomical Society* **498**, 2492 (2020).

[47] A. Tamone, A. Raichoor, C. Zhao, A. De Mattia, C. Gorgoni, E. Burtin, V. Ruhlmann-Kleider, A. J. Ross, S. Alam, W. J. Percival, *et al.*, *Monthly Notices of the Royal Astronomical Society* **499**, 5527 (2020).

[48] A. De Mattia, V. Ruhlmann-Kleider, A. Raichoor, A. J. Ross, A. Tamone, C. Zhao, S. Alam, S. Avila, E. Burtin, J. Bautista, *et al.*, *Monthly Notices of the Royal Astronomical Society* **501**, 5616 (2021).

[49] R. Neveux, E. Burtin, A. de Mattia, A. Smith, A. J. Ross, J. Hou, J. Bautista, J. Brinkmann, C.-H. Chuang, K. S. Dawson, *et al.*, *Monthly Notices of the Royal Astronomical Society* **499**, 210 (2020).

[50] J. Hou, A. G. Sánchez, A. J. Ross, A. Smith, R. Neveux, J. Bautista, E. Burtin, C. Zhao, R. Scoccimarro, K. S. Dawson, *et al.*, *Monthly Notices of the Royal Astronomical Society* **500**, 1201 (2021).

[51] F. Kirsten, B. Marcote, K. Nimmo, J. Hessels, M. Bhardwaj, S. Tendulkar, A. Keimpema, J. Yang, M. Snelders, P. Scholz, *et al.*, *Nature* **602**, 585 (2022).

[52] M. Bhardwaj, B. Gaensler, V. Kaspi, T. Landecker, R. Mckinven, D. Michilli, Z. Pleunis, S. Tendulkar, B. Andersen, P. Boyle, *et al.*, *The Astrophysical Journal Letters* **910**, L18 (2021).

[53] S. Bhandari, A. C. Gordon, D. R. Scott, L. Marnoch, N. Sridhar, P. Kumar, C. W. James, H. Qiu, K. W. Bannister, A. T. Deller, *et al.*, *The Astrophysical Journal* **948**, 67 (2023).

[54] A. C. Gordon, W.-f. Fong, C. D. Kilpatrick, T. Eftekhar, J. Leja, J. X. Prochaska, A. E. Nugent, S. Bhandari, P. K. Blanchard, M. Caleb, *et al.*, *The Astrophysical Journal* **954**, 80 (2023).

[55] C.-H. Niu, K. Aggarwal, D. Li, X. Zhang, S. Chatterjee, C.-W. Tsai, W. Yu, C. Law, S. Burke-Spoliar, J. Cordes, *et al.*, *Nature* **606**, 873 (2022).

[56] D. Foreman-Mackey, D. W. Hogg, D. Lang, and J. Goodman, *Publications of the Astronomical Society of the Pacific* **125**, 306 (2013).

[57] P. Mukherjee and N. Banerjee, *Physical Review D* **105**, 063516 (2022).

[58] G.-J. Wang, X.-J. Ma, and J.-Q. Xia, *Monthly Notices of the Royal Astronomical Society* **501**, 5714 (2021).

[59] M. Amiri, K. Bandura, A. Boskovic, T. Chen, J.-F. Cliche, M. Deng, N. Denman, M. Dobbs, M. Fandino, S. Foreman, *et al.*, *The Astrophysical Journal Supplement Series* **261**, 29 (2022).

[60] H. Qiu, E. F. Keane, K. W. Bannister, C. W. James, and R. M. Shannon, *Monthly Notices of the Royal Astronomical Society* **523**, 5109 (2023).

[61] J. Tian, K. Rajwade, I. Pastor-Marazuela, B. Stappers, M. C. Bezuidenhout, M. Caleb, F. Jankowski, E. Barr, and M. Kramer, *Monthly Notices of the Royal Astronomical Society* **533**, 3174 (2024).